JEMAT 2023, Vol 11, No 1, 25-31
https://doi.org/10.54987/jemat.v11i1.841

HIBISCUS PUBLISHER

JOURNAL OF ENVIRONMENTAL MICROBIOLOGY AND TOXICOLOGY

Website: http://journal.hibiscuspublisher.com/index.php/JEMAT/index

Substrate Inhibition Modelling of *Pseudomonas nitroreducens* Growth on Octylphenol Polyethoxylates

Abdusssamad Abubakar[1], Hafeez Muhammad Yakasai[2], Garba Uba[3] and Ibrahim Sabo[4]*

[1]National Environmental Standards and Regulations Enforcement Agency P. M. B. 641, Wuse Zone 7, NESREA, Abuja, FCT, Nigeria.
[2]Department of Biochemistry, Faculty of Basic Medical Sciences, College of Health Science, Bayero University Kano PMB 3011, Kano State, Nigeria.
[3]Department of Science Laboratory Technology, College of Science and Technology, Jigawa State Polytechnic, Dutse, PMB 7040, Nigeria.
[4]Department of Microbiology, Faculty of Pure and Applied Sciences, Federal University Wukari, P.M.B. 1020 Wukari, Taraba State, Nigeria.

*Corresponding author:
Ibrahim Alhaji Sabo
Department of Microbiology,
Faculty of Pure and Applied Sciences,
Federal University Wukari,
P.M.B. 1020 Wukari,
Taraba State,
Nigeria.
Email: ibrahimsabodzk@dzk.com

HISTORY

Received: 15th May 2023
Received in revised form: 15th July 2023
Accepted: 30th July 2023

KEYWORDS

Substrate Inhibition Models
Teissier
Pseudomonas nitroreducens
Octylphenol polyethoxylates
OPE-degrading bacterium

ABSTRACT

Octylphenol polyethoxylates (OPEs) constitute a class of non-ionic surfactants extensively employed in various industrial applications. However, concerns have arisen regarding the potential environmental and human health impacts of OPEs because of their widespread use and persistence in aquatic environments. Bioremediation of OPE in the environment using OPE-degrading bacterium is appealing as bacterial metabolism converts OPE to harmless carbon dioxide and water as byproducts. In this study, various secondary growth models such as Luong, Yano, Teissier-Edward, Aiba, Haldane, Monod, Han, and Levenspiel were employed to model the inhibitory effect of high OPE concentrations to the growth rate of *Pseudomonas nitroreducens* TX1 the bacterium on OPE. Following thorough statistical analyses such as root-mean-square error (RMSE), adjusted coefficient of determination (adjR^2), bias factor (BF), and accuracy factor (AF), the Teissier model emerged as the most optimal choice. All of the studied models showed good fittings except Moser, Monod and Hinshelwood which showed the poorest curve fitting. The Teissier model emerged as the most suitable model, as indicated by its remarkably low values for RMSE, AICc, and modified adjR^2. Furthermore, the model's AF and BF values were close to unity. The experimental data obtained indicates that OPE is toxic and slows down the rate of growth at higher concentrations. The maximum OPE specific growth rate (μ_{max}), half-saturation concentration (K_S), half inhibition concentration (K_i) was 0.613 h^{-1} (95% Confidence Interval or C.I. from 0.519 to 0.707), 2352.8 mg/L (95% C.I. from 1668.8 to 3036.8) and 52,456.7 mg/L (95% C.I. from 38395.0 to 66518.5), respectively. It is possible that these new constants found when modeling could be useful inputs for future modeling efforts.

INTRODUCTION

Octylphenol polyethoxylates (OPEs) find applications in various industrial processes due to their surfactant properties. They are utilized for emulsification, creating stable emulsions that aid in the mixing of substances that would typically separate, such as oil and water, proving valuable in industries like agriculture and cosmetics. OPEs also serve as effective wetting agents, enhancing the spreading and absorption of liquids on solid surfaces, making them useful in formulating agrochemicals, paints, and coatings. In the textile industry, OPEs function as surfactants for dyeing processes, dispersing dyes evenly and improving their penetration into fibers. Industrial cleaning products benefit from OPEs as their emulsifying and wetting properties facilitate the removal of dirt and contaminants [1].

Additionally, OPEs are employed in the paper and pulp industry as additives to improve the wetting and penetration of chemicals during pulping and papermaking processes. They play a role in agrochemical formulations, enhancing the distribution and effectiveness of active ingredients on crops. OPEs find application in metalworking fluids, improving lubrication and

cooling during machining processes by maintaining stable emulsions in water-based fluids [2]. Personal care products, such as shampoos and lotions, may contain OPEs due to their emulsifying and dispersing properties. In adhesives and sealants, OPEs contribute to improved wetting of surfaces, enhancing overall product performance. Furthermore, in polymer industries, OPEs may be utilized as emulsifiers in polymerization processes, aiding in the dispersion of polymer particles and stabilizing reactions. It's important to note that despite their widespread past use, concerns about the environmental and health impacts of OPEs have led to regulatory scrutiny. As a result, alternative, more environmentally friendly surfactants are being explored in various industries [3].

OPEs exhibit toxicity towards aquatic organisms like fish, algae, and invertebrates by disrupting cell membranes and affecting normal functioning. Accumulation in sediments and bioaccumulation in aquatic species pose long-term exposure risks, leading to potential ecological consequences [2,4–6]. A major concern is their capacity to function as endocrine disruptors, particularly with documented estrogenic activity that interferes with the endocrine system of aquatic organisms, resulting in reproductive abnormalities and compromised success in exposed organisms.

Despite well-documented environmental impacts, research also emphasizes potential human health risks associated with OPE exposure. These compounds can enter the human body through various pathways, raising concerns about their role in hormone regulation and the development of specific health conditions. Environmental monitoring and biomonitoring data, reviewed in a study assessing human exposure to nonylphenol (NP), indicate source-specific Margins of Exposure (MOEs) ranging from 2863 to 8.4 × 107, well above 1000, suggesting reasonable certainty of no harm for both source-specific and aggregate exposures to NP [1]).

In a study by Baldwin et al. [4], it was observed that nonylphenol polyethoxylate (NPPG) at 5.0 mg/liter inhibits testosterone elimination in Daphnia magna, mirroring the effects seen with its degradation product 4-nonylphenol. Interestingly, NPPG did not induce significant chronic toxicity, suggesting that environmental concentrations of NPPG may not pose a risk to invertebrates. Another investigation by TenEyck and Markee [5] focused on assessing the toxicity of three phenolic compounds—nonylphenol (NP), nonylphenol monoethoxylate (NP1EO), and nonylphenol diethoxylate (NP2EO)—to *Pimephales promelas* and *Ceriodaphnia dubia*. The study involved testing binary and tertiary mixtures, commonly found in surface waters due to wastewater discharges. The fathead minnows exhibited LC50 values of 136, 218, and 323 µg/L for NP, NP1EO, and NP2EO, respectively, indicating potential additive or synergistic effects in mixtures.

Furthermore, Song and Bielefeldt [6] explored the impact of five alkylphenol polyethoxylate nonionic surfactants on the microbial degradation of glucose and pentachlorophenol (PCP) by *Sphingomonas chlorophenolicum* RA2. The study revealed that surfactants with mid-range hydrophile–lipophile balance (HLB) values (13.5–15) were most compatible with substrate degradation. Interestingly, the lowest HLB surfactant inhibited RA2 growth, while the highest HLB surfactant showed inhibitory effects only at concentrations well above its critical micelle concentration (CMC).

The surfactants exhibited more inhibitory effects on RA2's PCP biodegradation compared to glucose, suggesting potential interactions with membrane-associated PCP-degrading enzymes [6]. These findings have practical implications for selecting surfactants in remedial applications involving biodegradation or oil dispersion. In a previous study, an OPE-degrading bacterium was isolated and characterized as an effort to remediate OPEs. The growth rate of the bacterium on OPE showed significant inhibition at high concentration of OPE.

MATERIALS AND METHODS

Data acquisition

The graphical data extracted from Figure 2 on the biodegradation of OPE by *Pseudomonas nitroreducens TX1* [7], was analyzed using the software tool Webplot digitizer. This software is widely acknowledged and embraced within the scientific community [8], for its capacity to convert scanned figures into digital data. Its precision and reliability have been consistently recognized by numerous researchers [9,10]. The data was further analyzed and modeled using Curve Expert Professional software (Version 2.6.5) to elucidate the scientific insights and trends within the dataset, contributing to the robustness of the study's findings. This combination of data digitization and advanced software analysis is a common and essential practice in modern scientific research, ensuring the accuracy and validity of results.

Fitting of the data

The Marquardt algorithm was employed for nonlinear regression to fit various bacterial growth models (**Table 1**) and this analysis was conducted using Curve Expert Professional software (Version 2.6.5). The algorithm aims to find the most optimal method for minimizing the sum of squares between predicted and observed values. In this process, the software can be configured manually or automatically to determine the initial parameter values, and the steepest gradient search between the four data points was utilized to estimate the maximum growth rate (μ_{max}).

Statistical analysis

The statistically significant difference between the models was evaluated using various metrics, The following statistical functions were utilized to determine the best models.

The RMSE allows number of parameters' penalty and was calculated using Equation 1, where n illustrates the number of experimental data, where else p is the number of parameters calculated by the model and experimental data and values predicted by the model are Ob_i and Pd_i, respectively [11]. With the regression line approaching the data points, the root mean square error (RMSE) reduces due to the reduced error in the model. More accurate predictions are generated by a model that has a lower error rate.

Comparable in magnitude to the dependent (outcome) variable, the RMSE values span an infinite number of positive infinities. The root mean square error (RMSE) can be employed to assess the extent of imprecision in a statistical model, including regression models. If a value is zero, it signifies that the predicted and actual values are an exact match. The model exhibits superior data fit and generates more precise predictions, as indicated by low RMSE values. In contrast, increased levels indicate a greater magnitude of errors and a reduced number of precise predictions.

Table 1. Substrate inhibition mathematical models.

Author	Degradation Rate	Author
Monod	$\frac{\mu_{max}S}{S+K_s}$	[12]
Haldane	$\frac{\mu_{max}S}{S+K_s+\left(\frac{S^2}{K_i}\right)}$	[13]
Teissier	$\mu_{max}\left(1-exp\left(-\frac{S}{K_i}\right)-exp\left(\frac{S}{K_s}\right)\right)$	[14]
Aiba	$\mu_{max}\frac{S}{K_s+S}exp\left(-\frac{S}{K_i}\right)$	[15]
Yano and Koga	$\frac{\mu_{max}S}{S+K_s+\left(\frac{S^2}{K_i}\right)\left(1+\frac{S}{K}\right)}$	[16]
Han and Levenspiel	$\mu_{max}\left(1-\left(\frac{S}{S_m}\right)\right)^n\left(\frac{S}{S+K_s\left(1-\left(\frac{S}{S_m}\right)\right)^m}\right)$	[17]
Luong	$\mu_{max}\frac{S}{S+K_s}\left(1-\left(\frac{S}{S_m}\right)\right)^n$	[18]
Moser	$\frac{\mu_{max}s^n}{K_s+s^n}$	[19]
Webb	$\frac{\mu_{max}S\left(1+\frac{S}{K}\right)}{S+K_s+\frac{S^2}{K_i}}$	[20]
Hinshelwood	$\mu_{max}\frac{S}{K_s+S}(1-K_pP)$	[21]

Note:
μ_{max} maximal specific growth rate
K_s half saturation constant
K_i inhibition constant
S_m maximal concentration of substrate tolerated
K_p product inhibition constant
m, n, K curve parameters
S substrate concentration
p product concentration

$$RMSE = \sqrt{\frac{\sum_{i=1}^{n}(Pd_i-Ob_i)^2}{n-p}} \quad \text{(Eqn. 1)}$$

The R^2 value, also known as the coefficient of determination, was used in linear regression to select the model that provided the best fit. On the other hand, in the case of nonlinear regression, the R^2 does not provide a comparative analysis in situations in which the number of parameters in the various models varies. In order to get around this obstacle, the quality of the nonlinear models was determined by adjusting the R^2 value. S_y^2 is the total variance of the y-variable, while RMS stands for residual mean square. These two terms are used in the adjusted R^2 formula (Equations 2 and 3).

$$Adjusted\ (R^2) = 1 - \frac{RMS}{S_Y^2} \quad \text{(Eqn. 2)}$$

$$Adjusted\ (R^2) = 1 - \frac{(1-R^2)(n-1)}{(n-p-1)} \quad \text{(Eqn. 3)}$$

One can measure the relative quality of various statistical models for a given set of experimental data by using the Akaike Information Criterion (AIC). This criterion was developed by Akaike. Instead, data sets that have a large number of parameters or few values should utilize the AIC that has been corrected, which is denoted by the letter AICc [22]. The AICc was determined using the equation that is presented below (Equation 4).

$$AICc = 2p + n1n\left(\frac{RSS}{n}\right) + 2(p+1) + \frac{2(p+1)(p+2)}{n-p-2} \quad \text{(Eqn. 4)}$$

Another statistical measure that is founded on information theory is known as the Bayesian Information Criterion (BIC) (Equation 5), which can be compared to the AICc. Models with the lowest Bayesian information criterion (BIC) are typically preferred over those with higher BICs when choosing from a finite number of models. It has close ties to the Akaike information criteria and is partially based on the likelihood function (AIC). This error function imposes a harsher penalty on the number of parameters than the AIC does [23].

$$BIC = n.\ln\frac{RSS}{n} + p.\ln(n) \quad \text{(Eqn. 5)}$$

The Hannan–Quinn information criterion, often known as the HQC, is an additional error function approach that is based on the information theory (Equation 7). To evaluate how well a statistical model fits data, experts use the Hannan-Quinn information criterion (HQC). It is a common metric to employ when choosing one model over another. In contrast to the LLF, it is connected to Akaike's information criterion. The HQC, like the AIC, includes a penalty function for the total number of model parameters, however it is significantly bigger than the value assigned by the AIC because the equation contains the *ln ln n* term [24];

$$HQC = n \times ln\frac{RSS}{n} + 2 \times p \times ln(\ln n) \quad \text{(Eqn. 7)}$$

Both BF and AF were utilized in an effort to evaluate the appropriateness of the models. In order to get a correlation of 1 between the anticipated value and the observed value, the Bias Factor needs to be equal to 1.

The Bias Factor and Accuracy Factor originates from predictive microbiology under the food microbiology field and have found applications in modelling microbial growth that leads to food spoilage [25–32]. A fail-safe model is indicated when the value of the Bias Factor (Equation 8) is greater than 1, and a fail-negative model is indicated when the value of the Bias Factor is less than 1. When compared to 1, a value of Accuracy that is less than 1 indicates a less accurate prediction (Equation 9).

$$Bias\ factor = 10\left(\sum_{i=1}^{n} log\frac{(Pd_i/Ob_i)}{n}\right) \quad \text{(Eqn. 8)}$$

$$Accuracy\ factor = 10\left(\sum_{i=1}^{n} log\frac{|(Pd_i/Ob_i)|}{n}\right) \quad \text{(Eqn. 9)}$$

Another parameter-penalized model is MPSD. The Marquardt's percent standard deviation (MPSD). This error function distribution follows the geometric mean error which allows for the penalty to the number of parameters of a model (Equation 10).

$$MPSD = 100\sqrt{\frac{1}{n-p}\sum_{i=1}^{n}\left(\frac{Ob_i-Pd_i}{Ob_i}\right)^2} \quad \text{(Eqn. 10)}$$

where p is the number of parameters, n is the number of experimental data, Ob_i is the experimental data, and Pd_i is the value predicted by the model.

RESULTS AND DISCUSSION

According to the analysis of the bacterial growth model, as depicted in **Figs. 1** to **7**., all of the studied models showed good fittings except Moser, Monod and Hinshelwood which showed the poorest curve fitting. The Teissier model emerged as the most suitable model, as indicated by its remarkably low values for RMSE, AICc, and modified adjR^2. Furthermore, the model's AF and BF values were close to unity (**Table 2)**. The experimental data obtained indicates that OPE is toxic and slows down the rate of growth at higher concentrations. The maximum OPE specific growth rate (μ_{max}), half-saturation concentration (K_S), half inhibition concentration (K_i) was 0.613 h^{-1} (95% Confidence Interval or C.I. from 0.519 to 0.707), 2352.8 mg/L (95% C.I. from 1668.8 to 3036.8) and 52,456.7 mg/L (95% C.I. from 38395.0 to 66518.5), respectively.

The Teissier model (or Tessier) is an extension of the Monod equation, which describes the rate of a microbiological reaction as a function of substrate concentration. The Teissier model introduces an additional parameter to account for substrate inhibition, a phenomenon where high substrate concentrations lead to a decrease in growth rate [14]. The Teissier model adapted for bacterial growth on toxic substances considers the impact of inhibitory effects of toxic compounds on microbial populations. Research in this area often involves assessing the impact of pollutants on microbial communities in contaminated environments. The Teissier model provides a means to understand how toxic substances influence bacterial growth dynamics, aiding in predicting the behavior of microbial populations under varying environmental conditions. The Teissier model has found excellent applications in other toxic compounds degradation by microorganisms such as in the degradation of nicosulfuron by a Pseudomonas nitroreducens strain NSA02 [33], anionic surfactant (SDS) degradation by immobilized mixed bacteria consortium [34], bioreduction rate of Chromium (VI) by Bacillus subtilis [35], degradation of Bisphenol A by Pseudomonas aeruginosa PAb1 isolated from the effluent of a thermal paper industry [36], degradation of asphaltene utilizing microorganisms isolated from oil samples [37], *Staphylococcus aureus* growth on Basic Violet 3 [38] and molybdenum reduction by bacterium [39].

Table 2. Statistical analysis of the substrate inhibition models utilized in this study.

Model	p	RMSE	adR^2	MPSD	AICc	BIC	HQC	BF	AF
Luong	4	0.0409	0.9198	19.967	-53.578	-71.639	-74.297	1.016	1.141
Yano	4	0.0355	0.9432	14.433	-56.995	-75.056	-77.713	1.015	1.106
Tessier-Edward	3	0.0318	0.9557	12.641	-66.499	-78.758	-80.752	1.004	1.110
Aiba	3	0.0371	0.9386	15.754	-62.799	-75.059	-77.052	1.001	1.122
Haldane	3	0.0348	0.9456	15.552	-64.326	-76.586	-78.579	1.023	1.122
Monod	2	0.1405	-1.7543	35.790	-36.289	-44.320	-45.648	1.132	1.472
Han and Levenspiel	5	0.0587	0.8513	12.954	-35.702	-62.077	-65.399	1.060	1.103
Moser	3	0.1404	-1.0630	36.692	-30.851	-43.111	-45.104	1.092	1.423
Hinshlewood	4	0.1571	-2.5414	40.015	-21.289	-39.350	-42.007	1.132	1.472
Webb	4	0.0369	0.9378	16.496	-56.040	-74.101	-76.759	1.023	1.122

Note: p is the number of parameters

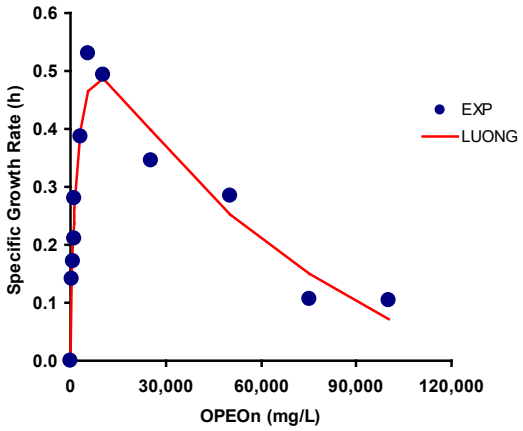

Fig. 1. Growth of *Pseudomonas nitroreducens TX1* modeled using Luong.

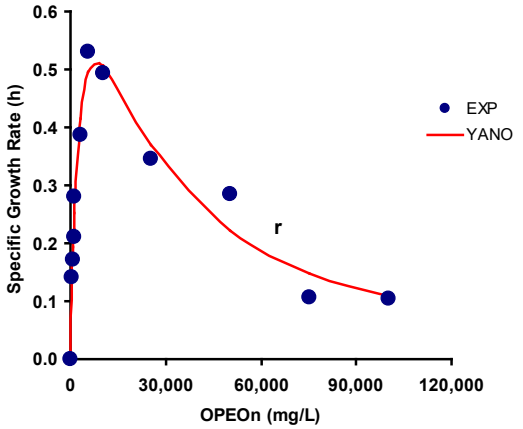

Fig. 2. Growth of Pseudomonas nitroreducens TX1 modeled using Yano.

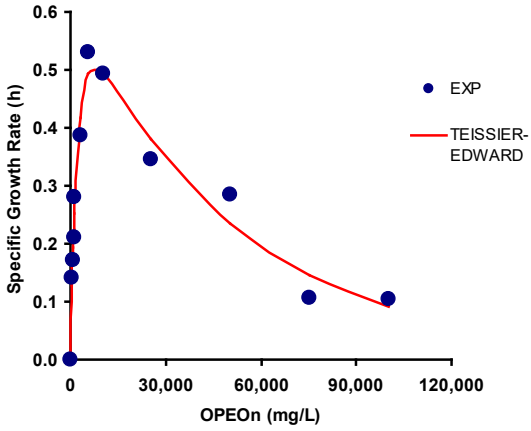

Fig. 3. Growth *of Pseudomonas nitroreducens TX1* modeled using Teissier- Edward.

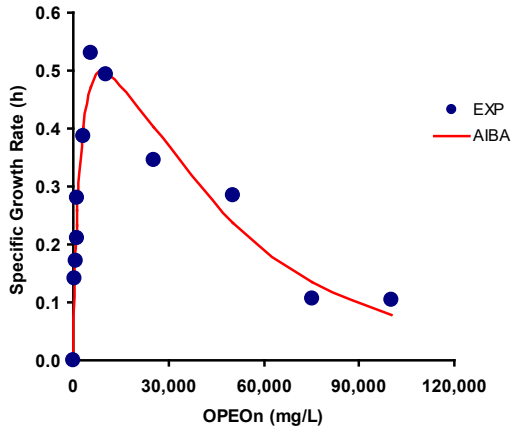

Fig. 4. Growth of *Pseudomonas nitroreducens TX1* modeled using Aiba.

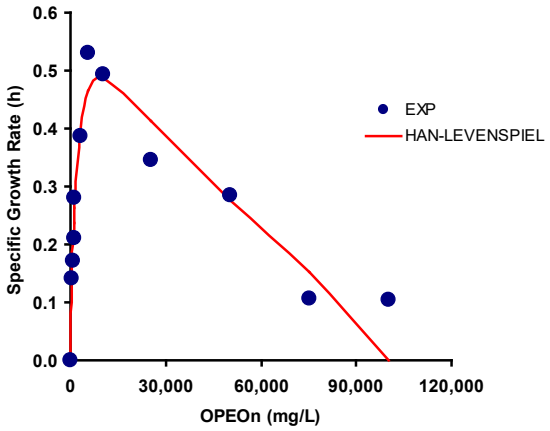

Fig. 7. Growth of *Pseudomonas nitroreducens TX1* modeled using Han-Levenspiel.

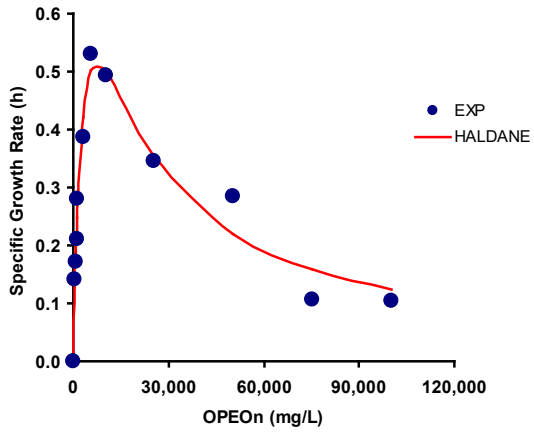

Fig. 5. Growth of *Pseudomonas nitroreducens TX1* modeled using Haldane.

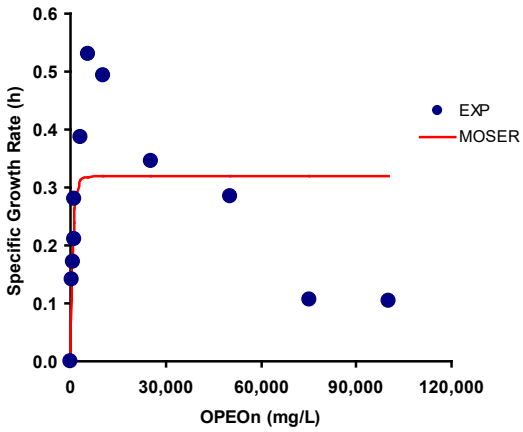

Fig. 8. Growth of *Pseudomonas nitroreducens TX1* modeled using Moser.

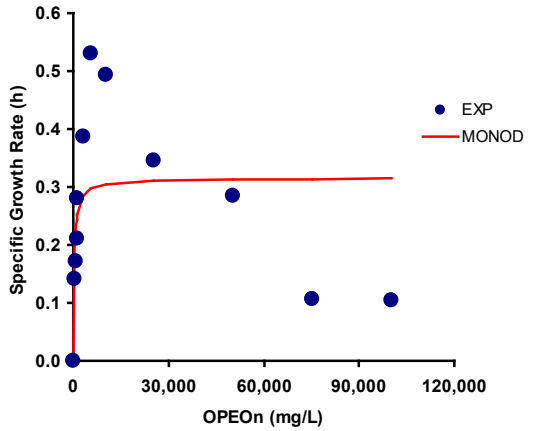

Fig. 6. Growth of *Pseudomonas nitroreducens TX1* modeled using Monod.

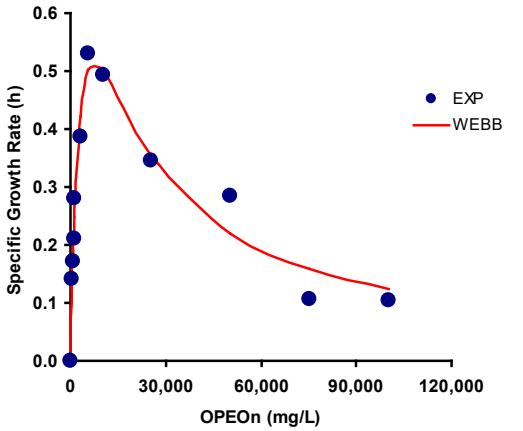

Fig. 9. Growth of *Pseudomonas nitroreducens TX1* modeled using Webb.

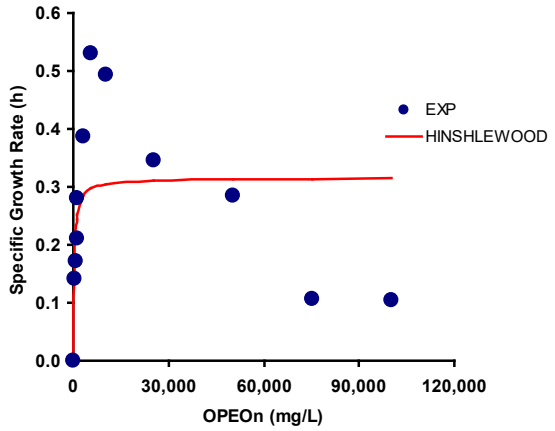

Fig. 10. Growth of *Pseudomonas nitroreducens TX1* modeled using Hinshelwood.

Practically, the biologically significant coefficients derived from this analysis hold substantial value for guiding and optimizing both batch and field experiments. These coefficients provide a valuable tool for researchers and environmental scientists, enabling precise predictions concerning the growth conditions and requirements of *Pseudomonas nitroreducens* TX1 in the context of remediating Octylphenol Polyethoxylates (OPE) in polluted environments.

Notably, employing a substrate inhibition kinetics model to assess the impact of toxic compounds on microbial growth or degradation rates is gaining recognition as a crucial practice. While many studies traditionally lean towards either the Haldane or Monod models for modeling purposes, a select few, including this study, adopt a comprehensive modeling approach to leverage the flexibility offered by alternative models. The utilization of such a comprehensive approach not only yields improved curve fitting results compared to a few popular models but also represents a more nuanced and thorough strategy for understanding the dynamics of microbial responses to toxic compounds.

CONCLUSION

In conclusion, after conducting a comprehensive analysis that included various statistical metrics such as the corrected AICc (Akaike Information Criterion), bias factor (BF), adjusted coefficient of determination (R^2), and root-mean-square error (RMSE), it has been determined that the Teissier model stands out as the most suitable model for describing the growth of the bacterium on OPE. This model's superiority was clearly evident through these statistical assessments. From the fitting exercise, we were able to extract valuable parameters for the model. The maximum OPE specific growth rate (μ_{max}), half-saturation concentration (K_S), half inhibition concentration (K_i) was 0.613 h^{-1} (95% Confidence Interval or C.I. from 0.519 to 0.707), 2352.8 mg/L (95% C.I. from 1668.8 to 3036.8) and 52,456.7 mg/L (95% C.I. from 38395.0 to 66518.5), respectively. This knowledge will be instrumental in designing effective strategies for addressing environmental contamination and further advancing our understanding of microbial processes in environmental remediation.

REFERENCES

1. Osimitz TG, Droege W, Driver JH. Human Risk Assessment for Nonylphenol. Hum Ecol Risk Assess Int J. 2015 Oct 3;21(7):1903–19.
2. Schüürmann G. Acute aquatic toxicity of alkyl phenol ethoxylates. Ecotoxicol Environ Saf. 1991 Apr 1;21(2):227–33.
3. Yan B, Luo L, Yang H. Isolation and characterization of Aeromonas sp. TXBc10 capable of high-efficiency degradation of octylphenol polyethoxylate from tannery wastewater. Environ Technol. 2020 Dec 18;41(28):3722–31.
4. Baldwin WS, Graham SE, Shea D, LeBlanc GA. Altered Metabolic Elimination of Testosterone and Associated Toxicity Following Exposure ofDaphnia magnato Nonylphenol Polyethoxylate. Ecotoxicol Environ Saf. 1998 Feb 1;39(2):104–11.
5. TenEyck MC, Markee TP. Toxicity of Nonylphenol, Nonylphenol Monoethoxylate, and Nonylphenol Diethoxylate and Mixtures of these Compounds to Pimephales promelas (Fathead Minnow) and Ceriodaphnia dubia. Arch Environ Contam Toxicol. 2007 Nov 1;53(4):599–606.
6. Song M, Bielefeldt AngelaR. Toxicity and inhibition of bacterial growth by series of alkylphenol polyethoxylate nonionic surfactants. J Hazard Mater. 2012 Jun 15;219–220:127–32.
7. Chen HJ, Guo GL, Tseng DH, Cheng CL, Huang SL. Growth factors, kinetics and biodegradation mechanism associated with Pseudomonas nitroreducens TX1 grown on octylphenol polyethoxylates. J Environ Manage. 2006 Sep 1;80(4):279–86.
8. Rohatgi A. WebPlotDigitizer User Manual 4.3. HttparohatgiinfoWebPlotDigitizerapp Accessed June 2 2014. 2020;1–17.
9. Yahuza S, Dan-iya BI, Sabo IA. Modelling the Growth of Enterobacter sp . on Polyethylene. J Biochem Microbiol Biotechnol. 2020;8(1):42–6.
10. Sabo IA, Yahuza S, Shukor MY. Molybdenum Blue Production from Serratia sp. strain DRY5: Secondary Modeling. Bioremediation Sci Technol Res. 2021;9(2):21–4.
11. Wayman M, Tseng MC. Inhibition-threshold substrate concentrations. Biotechnol Bioeng. 1976;18(3):383–7.
12. Monod J. The Growth of Bacterial Cultures. Annu Rev Microbiol. 1949;3(1):371–94.
13. Boon B, Laudelout H. Kinetics of nitrite oxidation by Nitrobacter winogradskyi. Biochem J. 1962;85:440–7.
14. Teissier G. Growth of bacterial populations and the available substrate concentration. Rev Sci Instrum. 1942;3208:209–14.
15. Aiba S, Shoda M, Nagatani M. Kinetics of product inhibition in alcohol fermentation. Biotechnol Bioeng. 1968 Nov 1;10(6):845–64.
16. Yano T, Koga S. Dynamic behavior of the chemostat subject to substrate inhibition. Biotechnol Bioeng. 1969 Mar 1;11(2):139–53.
17. Han K, Levenspiel O. Extended Monod kinetics for substrate, product, and cell inhibition. Biotechnol Bioeng. 1988;32(4):430–7.
18. Luong JHT. Generalization of monod kinetics for analysis of growth data with substrate inhibition. Biotechnol Bioeng. 1987;29(2):242–8.
19. Moser A. Kinetics of batch fermentations. In: Rehm HJ, Reed G, editors. Biotechnology. VCH Verlagsgesellschaft mbH, Weinheim; 1985. p. 243–83.
20. Webb JLeyden. Enzyme and metabolic inhibitors [Internet]. New York: Academic Press; 1963. 984 p. Available from: https://www.biodiversitylibrary.org/bibliography/7320
21. Hinshelwood CN. The chemical kinetics of the bacterial cell. Clarendon Press, Gloucestershire, UK; 1946.
22. Akaike H. Making statistical thinking more productive. Ann Inst Stat Math. 2010;62(1):3–9.
23. Kass RE, Raftery AE. Bayes Factors. J Am Stat Assoc. 1995 Jun 1;90(430):773–95.
24. Burnham KP, Anderson DR. Model Selection and Multimodel Inference: A Practical Information-Theoretic Approach. Springer Science & Business Media; 2002. 528 p.
25. Ross T, McMeekin TA. Predictive microbiology. Int J Food Microbiol. 1994;23(3–4):241–64.
26. Zhou K, George SM, Métris A, Li PL, Baranyi J. Lag phase of Salmonella enterica under osmotic stress conditions. Appl Environ Microbiol. 2011;77(5):1758–62.

27. Zhao J, Gao J, Chen F, Ren F, Dai R, Liu Y, et al. Modeling and predicting the effect of temperature on the growth of *Proteus mirabilis* in chicken. J Microbiol Methods. 2014;99(1):38–43.
28. Velugoti PR, Bohra LK, Juneja VK, Huang L, Wesseling AL, Subbiah J, et al. Dynamic model for predicting growth of Salmonella spp. in ground sterile pork. Food Microbiol. 2011;28(4):796–803.
29. McElroy DM, Jaykus LA, Foegeding PM. Validation and analysis of modeled predictions of growth of Bacillus cereus spores in boiled rice. J Food Prot. 2000;63(2):268–72.
30. Kowalik J, Lobacz A, Tarczynska AS, Ziajka S. Graphie validation of growth models for Listeria monocytogenes in milk during storage. Milchwissenschaft. 2012;67(1):38–42.
31. Jung SH, Park SJ, Chun HH, Song KB. Effects of combined treatment of aqueous chlorine dioxide and fumaric acid on the microbial growth in fresh-cut paprika (capsicum annuum L.). J Appl Biol Chem. 2014;57(1):83–7.
32. Huang L, Hwang CA, Phillips J. Evaluating the Effect of Temperature on Microbial Growth Rate-The Ratkowsky and a Bělehrádek-Type Models. J Food Sci. 2011;76(8):M547–57.
33. Zhao H, Zhu J, Liu S, Zhou X. Kinetics study of nicosulfuron degradation by a Pseudomonas nitroreducens strain NSA02. Biodegradation. 2018;29(3):271–83.
34. Najim AA, Ismail ZZ, Hummadi KK. Immobilization of mixed bacteria by novel biocarriers extracted from Cress and Chia seeds for biotreatment of anionic surfactant (SDS)-bearing real wastewaters. Prep Biochem Biotechnol. 2022;
35. Basu S, Dasgupta M, Chakraborty B. Removal of Chromium (VI) by *Bacillus subtilis* Isolated from East Calcutta Wetlands, West Bengal, India. 2014;
36. Vijayalakshmi V, Senthilkumar P, Mophin-Kani K, Sivamani S, Sivarajasekar N, Vasantharaj S. Bio-degradation of Bisphenol A by *Pseudomonas aeruginosa* PAb1 isolated from effluent of thermal paper industry: Kinetic modeling and process optimization. J Radiat Res Appl Sci. 2018 Jan 1;11(1):56–65.
37. Tavassoli T, Mousavi SM, Shojaosadati SA, Salehizadeh H. Asphaltene biodegradation using microorganisms isolated from oil samples. Fuel. 2012 Mar 1;93:142–8.
38. Manogaran M, Habib NMSA, Shukor MY, Yasid NA. Mathematical Modeling of Substrate Inhibition Kinetics of Staphylococcus aureus Growth on Basic Violet 3. Bioremediation Sci Technol Res. 2022 Dec 31;10(2):50–5.
39. Halmi MIE, Abdullah SRS, Johari WLW, Ali MSM, Shaharuddin NA, Khalid A, et al. Modelling the kinetics of hexavalent molybdenum (Mo6+) reduction by the Serratia sp. strain MIE2 in batch culture. Rendiconti Lincei. 2016 Dec 1;27(4):653–63.